
HIM 1990-2015

2015

Using Antenna Tile-Assisted Substrate Delivery to Improve Detection Limits of Deoxyribozyme

Amanda J. Cox
University of Central Florida



Part of the [Biochemistry Commons](#)

Find similar works at: <https://stars.library.ucf.edu/honorstheses1990-2015>

University of Central Florida Libraries <http://library.ucf.edu>

This Open Access is brought to you for free and open access by STARS. It has been accepted for inclusion in HIM 1990-2015 by an authorized administrator of STARS. For more information, please contact STARS@ucf.edu.

Recommended Citation

Cox, Amanda J., "Using Antenna Tile-Assisted Substrate Delivery to Improve Detection Limits of Deoxyribozyme" (2015). *HIM 1990-2015*. 1861.

<https://stars.library.ucf.edu/honorstheses1990-2015/1861>



USING ANTENNA TILE-ASSISTED SUBSTRATE DELIVERY TO IMPROVE
THE DETECTION LIMITS OF DEOXYRIBOZYME BIOSENSORS

by

AMANDA J. COX

A thesis submitted in partial fulfillment of the requirements
for the Honors in the Major Program in Chemistry, Biochemistry Track
in the College of Sciences
and in the Burnett Honors College
at the University of Central Florida
Orlando, Florida

Fall Term, 2015

Thesis Chair: Dr. Dmitry Kolpashchikov, PhD

ABSTRACT

One common limitation of enzymatic reactions is the diffusion of a substrate to the enzyme active site and/or the release of the reaction products. These reactions are known as diffusion – controlled. Overcoming this limitation may enable faster catalytic rates, which in the case of catalytic biosensors can potentially lower limits of detection of specific analyte. Here we created an artificial system to enable deoxyribozyme (Dz) 10-23 based biosensor to overcome its diffusion limit. The sensor consists of the two probe strands, which bind to the analyzed nucleic acid by Watson-Crick base pairs and, upon binding re-form the catalytic core of Dz 10-23. The activated Dz 10-23 cleaves the fluorophore and quencher-labeled DNA-RNA substrate which separates the fluorophore from the quencher thus producing high fluorescent signal. This system uses a Dz 10-23 biosensor strand associated to a DNA antenna tile, which captures the fluorogenic substrate and channels it to the reaction center where the Dz 10-23 cleaves the substrate. DNA antenna tile captures fluorogenic substrate and delivers it to the activated Dz 10-23 core. This allows for lower levels of analyte to be detected without compromising the specificity of the biosensor. The results of this experiment demonstrated that using DNA antenna, we can create a synthetic environment around the Dz 10-23 biosensor to increase its efficiency and allow for lower levels of analyte to be detected without using amplification techniques like PCR.

ACKNOWLEDGEMENTS

I would like to thank Dr. Dmitry Kolpashchikov for all his guidance and expertise in helping me design, refine, and implement this project. As well as Dr. Kyle Rohde and Dr. Eda Koculi for their knowledge in refining this project. And I would like to thank all of the DK lab group members, who helped critique this project.

TABLE OF CONTENTS

CHAPTER ONE: BACKGROUND	1
CHAPTER TWO: RESULTS	6
Designing the Environment	6
Confirming the LOD of Sensor Dissolved in Solution	10
Testing the Tile Format	12
Checking Selectivity.....	15
Testing the Tile with RNA	18
SUMMARY	20
LIST OF REFERENCES	21

LIST OF FIGURES

Figure 1 Designs of deoxyribozyme 10-23 tested by Mokany et al. ^[3] a) The deoxyribozyme 10-23 core split into two pieces (light blue and dark blue) with the substrate (S) shown in green, the assembly factor (AF) shown in red, and the stabilizer arm (SA) shown in orange, hybridizing to form the Dz catalytic core. b) The AF is split into two pieces, AF (1) in red and AF (2) in orange and both are needed to reform the Dz catalytic core. c) The cascade of two MNAzymes happens as the substrate from MNAzyme 1 called: S1 and AF (2), shown in green and orange, is cleaved and then provides the second AF piece, which is needed by MNAzyme 2 to recombine the Dz catalytic core and cleave S2. d) When S1 and AF (2) is not cleaved by MNAzyme 1, it acts as an inhibitor for MNAzyme 2, preventing the hybridization of the catalytic core.	3
Figure 2 The structure of 10-23 deoxyribozyme isolated by Santoro and Joyce in 1997. The arrow indicates where the RNA strand is cleaved. Bases shown are conserved sequence.	4
Figure 3 Shows the general reaction mechanism between an enzyme and its substrate. The diffusion limitations occur at k_1 and/or k_3	4
Figure 4. Deoxyribozyme (Dz) 10-23 associated on tile. DZ_b of Dz 10-23 is in the center attached to the tile by the middle, purple strand while DZ_a (Not shown) is dissolved in solution. Orange strands indicate nucleotide sequences (16 total) where the hooks can hybridize to the tile. Hooks not shown.	7
Figure 5 A) Reaction scheme of Dz 10-23 biosensor. DZ_b and the substrate are dissolved in solution. When DZ_a and the analyte are added to the solution, the analyte binds to the analyte binding arms (dotted lines). This brings the Dz reaction core together allowing for the substrate to bind, be cleaved by the Dz biosensor, and then fluoresce as the fluorophore and quencher separate. B) Arrangement of the Dz 10-23 biosensor on the antenna tile. DZ_b is attached to the tile by the analyte binding arms while substrate (shown by Q—F strands) is attached to hooks (not shown) on the tile and concentrated around the reaction center. Addition of DZ_a and analyte brings the Dz core together allowing for the substrate to bind, be cleaved by the Dz biosensor, and then fluoresce as the fluorophore and quencher separate.	8

Figure 6 Native Gel electrophoresis of the samples. Lane 1 is the 100bp DNA ladder. Lane 2 is the Dz tile at 100 nM without Tdz5 (**DZ_b** of enzyme) and no hooks. Lane 3 is the full Dz tile at 100 nM with no hooks. Lane 4 is the full Dz tile at 100 nM with releasing hook at 160 nM. Lane 5 is the full Dz tile at 100 nM with delivering hook at 160 nM. Lane 6 is the full Dz tile at 100 nM with Mtb at 100 nM. 9

Figure 7 Deoxyribozyme 10-23 was dissolved in solution as two pieces. **DZ_a** concentration was 2 nM, **DZ_b** concentration was 10 nM, and F-substrate concentration was 200 nM. A) Absorbance at 517 nm of the sensor after 1 hr. of incubation at 55°C in the presence of various Mtb analyte concentrations. Limit of detection was 25.68 pM. B) Absorbance at 517nm of the sensor after 3 hrs. of incubation at 55°C in the presence of various Mtb analyte concentrations. Limit of detection was 4.07 pM. For both, the dashed lines show trendlines. Data are averages from three independent experiments and error bars show standard deviation. Solid line indicates threshold limits. 11

Figure 8 Deoxyribozyme 10-23 was dissolved in solution as two pieces. **DZ_a** concentration was 2 nM, **DZ_b** on the tile concentration was 10 nM, and 1S-Hook substrate concentration was 200 nM. Absorbance at 517 nm of the sensor after 1 hr. and 3 hrs. of incubation at 55°C respectively in the presence of various Mtb analyte concentrations. Dashed lines show treadlines. Data are averages from three independent experiments and error bars show standard deviation. Solid line indicates threshold limits. The Limit of detection was 2.31 pM after 1 hr. and 0.51 pM after 3 hrs. 13

Figure 9 Deoxyribozyme 10-23 trendline comparisons after 3 hrs incubation at 55°C. **DZ_a** concentration was 2 nM, **DZ_b** concentration was 10 nM, Hook concentrations were both at 160 nM, and substrate concentration was 200 nM. Absorbance at 517 nm of the sensor was measured in presence of various Mtb analyte concentrations. Data are averages from three independent experiments and error bars show standard deviation. Free sensor in solution (Blue), Dz Tile with No Hooks (Yellow), and Dz Tile with both the **delivering hook** and **releasing hook** (Red)..... 14

Figure 10 Limit of detection for sensor 2 dissolved in solution verses tile-associated Dz sensor 2 after 1 hr and 3 hrs. **M. smeg** **DZ_a** concentration was 2 nM, **M. smeg** **DZ_b** tile concentration was 10 nM, and substrate concentration was 200 nM. A) Absorbance at 517 nm of the sensor after 1 hr of incubation at 55°C in presence of various M. smeg analyte concentrations. Limit of detection was 15.21 pM for the sensor in solution and 11.63 pM on tile. B) Absorbance at 517 nm of the

sensor after 1 hr of incubation at 55°C in presence of various *M. smeg* analyte concentrations. Limit of detection was 6.40 pM in solution and 1.91 pM on tile. For both experiments, data are averages from three independent experiments and error bars show standard deviation..... 16

Figure 11 Shows the specificity of the Dz tile to its analyte Mtb and of Dz *M. smeg* tile to its analyte *M. smeg*. On the left is sensor 1 (*Mtb* sensitive biosensor) and on the right is sensor 2 (*M. smeg* sensitive biosensor). When sensor 1 is incubated with 100 pM of its matched analyte (*Mtb*, shown in green) for 1 hr, there is greater fluorescence than when sensor 1 was incubated with 100 pM of its mismatched analyte (*M. smeg*, shown in blue). For sensor 2, when incubated with its matched analyte (*M. smeg*) for 1 hr at 100 pM, there is greater fluorescence compared to when sensor 2 was incubated with its mismatched analyte (*Mtb*) for 1 hr at 100 pM. 17

Figure 12 Shows the fluorescence measurements of the Dz tile with RNA analyte compared to the sensor dissolved in solution with the RNA analyte. The **DZ_a** was at 2 nM, **DZ_b** was at 10 nM and attached to the tile, hook concentrations were both at 160 nM, the substrate was at 200 nM, and the RNA analyte concentration varied. A) Sample was incubated at 55°C and the fluorescence at 517 nm read after 1hr. The limit of detection of the biosensor dissolved in solution was 24.73 pM and on tile was 38.46 pM. B) Sample was incubated at 55°C and the fluorescence at 517 nm read after 3hrs. The limit of detection of the biosensor dissolved in solution was 11.97 pM and on tile was 6.40 pM. For both experiments, the data is an average of three experiments and the standard deviation is represented by the error bars. 19

Figure 13 Shows the limits of detections after 3 hrs of incubation at 55°C for each experiment with a gradient showing the best and worst. From these experiments we can see that the tile format reduces the limits of detection. 20

CHAPTER ONE: BACKGROUND

In 1994, Breaker and Joyce successfully isolated the first deoxyribozyme (also called DNAzyme, catalytic DNA, and Dz).^[1] Previously known enzymes were represented only by proteins or RNA, but by using *in vitro* selection or SELEX techniques, Breaker and Joyce were able to isolate an enzyme made of DNA that could catalyze the Pb²⁺-dependent cleavage of an RNA phosphoester bond.^[1] Since then, the knowledge about DNAzymes and the areas where we can apply them have increased drastically. In their review, Schlosser and Li explore what recent publications have discovered including the comparisons of DNAzymes with RNAzymes and proteins, and the potential roles that DNAzymes can play *in vivo* and *in vitro*.^[2] Some of the benefits of DNAzyme are that they are very stable, small in size, have a relatively high activity and multiple turnover, have very specific substrate selection, are versatile in substrate recognition, and are relatively low in cost.^[1,2] While both RNA and DNA are similar in structure and functional plasticity allowing for very specific selection of substrate and relatively easy preparation, DNAzymes are less sensitive to chemical degradation and can be directly amplified by PCR if needed.^[2,5] Compared to polypeptide enzymes, DNAzymes are more stable at room temperature, are smaller, and are easier to build since the interactions are predictable through Watson-Crick base pairs.^[2,5] On top of this, DNAzymes still have comparable rates of catalytic efficiency to their enzymatic competitors, especially with Dz 10-23 which is considered catalytically “perfect”.^[5,6,9] This notion will be explained in detail in later paragraphs. Recent studies have found a variety of DNAzymes that catalyze a range of reactions including cleavage, ligation, phosphorylation, deglycosylation, and branching of DNA and RNA, and DNA coupling, DNA depurination, and RNA lariat formation.^[2,3] The applications of DNAzymes have only just begun and include everything from diagnostic techniques and therapeutic applications to computational functions with logic gates and molecular switches to analysis of gene functions and structure.^[2-7] In their review, Dass *et al.* cover how DNAzymes could even be used in cancer treatment, gene therapy, and targeted therapy through light induced activation.^[10]

In 2001, Stojanovic *et al.* used deoxyribozymes to create a catalytic molecular beacon that could distinguish between any two single-stranded oligonucleotide sequences.^[11] They accomplished this by using the hybridization of the molecular beacon to the specific oligonucleotide sequence as a stabilizing effect. The stabilized molecular deoxyribozyme would then initiate the catalytic core, causing cleavage of a fluorophore and quencher labeled DNA-RNA substrate and separation of the fluorophore (5' terminus) and acceptor (3' terminus). When the target sequence was not present, the beacon module domain folded over the deoxyribozyme substrate recognition site and inhibited catalysis.^[11] Since then, deoxyribozyme biosensors were developed to have lower background fluorescence by splitting the DNAzymes into pieces.^[13] This effectively inhibits the catalytic core until it is recombined to form the MNAzyme (multicomponent nucleic acid enzyme) through the hybridization of the necessary pieces. In their research, Mokany *et al.* tested various ways to design a MNAzyme from deoxyribozyme 10-23.^[3] All of the designs in Figure 1 had the DNAzyme split into two pieces where each piece had substrate binding arms and assembly facilitator binding arms on either side of the catalytic core. The assembly facilitator binding arm is a nucleic acid sequence that was reverse complement to the assemble facilitator sequence. The presence of the assemble facilitator sequence allows for the Dz pieces to assemble back together and reform the core. For Figure 1a, the assembly facilitator binding arm was shortened on one of the DNAzyme pieces creating the need for a stabilizer arm. With this design, the solution needed both pieces of the DNAzyme, the substrate, the assembly factor, and the stabilizing arm in order to cleave the substrate, otherwise they saw no catalytic activity.^[3] Figure 1b shows another design of the MNAzyme, where they split the assembly facilitator itself into two pieces, and so both were needed in order to see catalytic activity. Figure 1c shows a cascade of two MNAzymes where the cleaved substrate from the first enzyme became the second half of the assembly factor for the second MNAzyme. Therefore, the first MNAzyme specifically regulated the activity of the second enzyme as shown in Figure 1d. They also designed it so that the first substrate, when un-cleaved, acted as an inhibitor to the second MNAzyme, see Figure 1d.^[3]

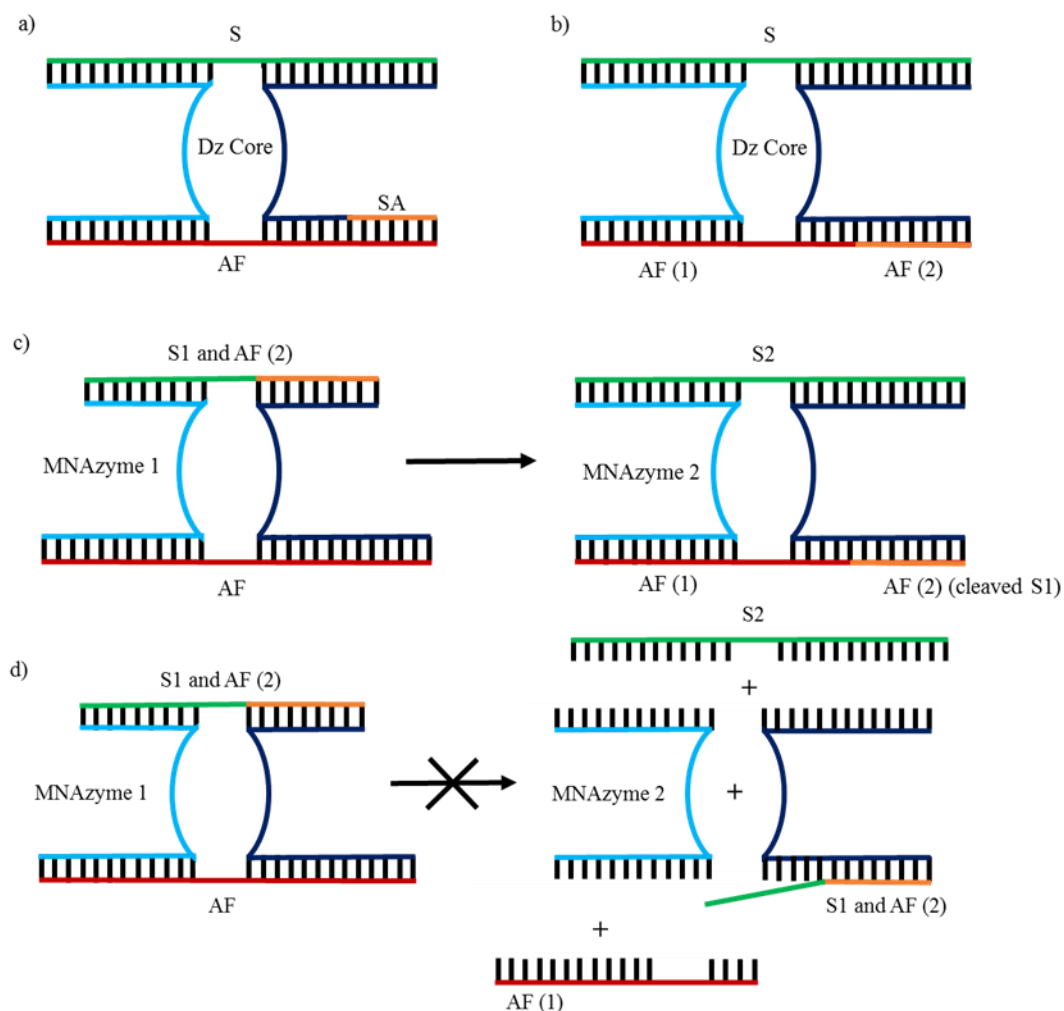


Figure 1 Designs of deoxyribozyme 10-23 tested by Mokany et al. [3] a) The deoxyribozyme 10-23 core split into two pieces (light blue and dark blue) with the substrate (S) shown in green, the assembly factor (AF) shown in red, and the stabilizer arm (SA) shown in orange, hybridizing to form the Dz catalytic core. b) The AF is split into two pieces, AF (1) in red and AF (2) in orange and both are needed to reform the Dz catalytic core. c) The cascade of two MNAszymes happens as the substrate from MNAszyme 1 called: S1 and AF (2), shown in green and orange, is cleaved and then provides the second AF piece, which is needed by MNAszyme 2 to recombine the Dz catalytic core and cleave S2. d) When S1 and AF (2) is not cleaved by MNAszyme 1, it acts as an inhibitor for MNAszyme 2, preventing the hybridization of the catalytic core.

Figure 1c and 1d show a cascade of MNAszymes where a specific input could have a specific output and create a molecular switch where “on” was the activated MNAszyme and “off” was the deactivated MNAszyme. This design has been adapted and applied practically in diagnostic techniques where the presence of a specific analyte, like an rRNA strand of HIV or *Mycobacterium*

tuberculosis, provides a specific output signal (i.e. fluoresce, colored product).^[4] This application of DNazymes could potentially expedite point-of-care diagnosis of diseases or monitor environmental or food contaminations. While beneficial in many ways, these deoxyribozyme sensors are limited by their ability to detect low levels of the target sequence/analyte/assemble facilitator/etc. In order to push these biosensors into real world appliances, it is essential to improve their detection limits.

This project takes advantage of the catalytic efficiency of deoxyribozyme (Dz) 10-23 shown in Figure 2, which was isolated and characterized by Santoro and Joyce.^[5]

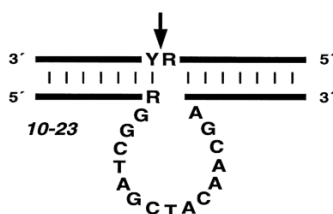


Figure 2 The structure of 10-23 deoxyribozyme isolated by Santoro and Joyce in 1997. The arrow indicates where the RNA strand is cleaved. Bases shown are conserved sequence.

This DNzyme behaves similarly to the hammerhead ribozyme in its need for a divalent metal cation in order to be active, but it has a catalytic efficiency (k_{cat}/K_m) = $10^9 \text{ M}^{-1} \cdot \text{min}^{-1}$ which greatly exceeds the catalytic efficiency of any other known nucleic acid enzyme.^[6,5] The reaction rate of deoxyribozyme 10-23 is comparable to the efficiency of some ribozymes.^[1,2,5,9] Through their experiments, Santoro and Joyce found that Dz 10-23 is catalytically perfect which is also known as diffusion limited.^[6] This means that how quickly the rate of the reaction proceeds, is determined by how quickly the enzyme and substrate can bind together (also known as k_1). In some cases, diffusion limited can also refer to how quickly the enzyme and product dissociate (also known as k_3). See Figure 3.

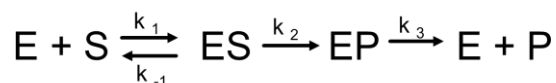


Figure 3 Shows the general reaction mechanism between an enzyme and its substrate. The diffusion limitations occur at k_1 and/or k_3 .

In nature, the diffusion limit is overcome by substrate channeling, like with pyruvate dehydrogenase.^[12] To mimic the natural substrate channeling, Fu *et al.* designed a NAD⁺-modified swinging arm on a DNA nanostructured platform that channeled a hydride between glucose-6-phosphate dehydrogenase (G6pDH) and malic dehydrogenase (MDH) providing restricted diffusion.^[7] They found that they were able to greatly enhance the activity of these enzymes as well as enable high selectivity in a complex environment. They also determined that by placing several swinging arms around the enzymes, they were able to increase the local concentration of NAD⁺ around the enzymes and saw an increase in their normalized activity.^[7]

Together, these ideas build the notion for designing an enzymatic complex system that optimizes the reaction conditions around the DNAzyme to theoretically increase k_1 and k_3 and thereby increase the efficiency of current DNAzymes and lower detection limits of Dz biosensors. We propose two methods to optimize the reaction conditions. The first being the localization of substrate around the Dz 10-23 and the second by creating “**hooks**” that channel substrate to the reaction center. With this design, we are looking to see lower levels of a target sequence to be detected. This is a critical step in pushing deoxyribozymes into real world applications as biosensors for diagnostic tests in the field, which is the ultimate goal of this project.

CHAPTER TWO: RESULTS

Designing the Environment

The focus of this design is two-fold. First, to localize the substrate around the Dz 10-23 by using a combination of nucleotide sequences that have affinity to the substrate, which we will refer to as ‘**hooks**’. The second is for these hooks to act as “swinging arms” to channel the substrate onto and off of the Dz reaction site. The design we created has two variations of hooks. The first is called the **delivering hook**, which helps localize the substrate right next to the enzyme and theoretically lower the diffusion limitation in k_1 . The second hook is called the **releasing hook** and it has affinity to the cleaved substrate, which can theoretically lower diffusion limitation in k_3 .

To start this design, we built a platform (also called a tile) using DNA nanotechnology techniques. Since the Dz 10-23 biosensor is split into two pieces (called **DZ_a** and **DZ_b**), we placed only one half (specifically **DZ_b**) in the center of the tile of DNA while **DZ_a** was dissolved in solution. Figure 4 shows this format. You will notice that the beginning and end of each DNA strand has a sequence in orange. This sequence of nucleotides is the reverse complement of half of the sequence on our hook strands. This allowed for variations of hooks to be tested without changing the main tile platform as well as random attachment with the **delivering hooks** and **releasing hooks** onto the tile.

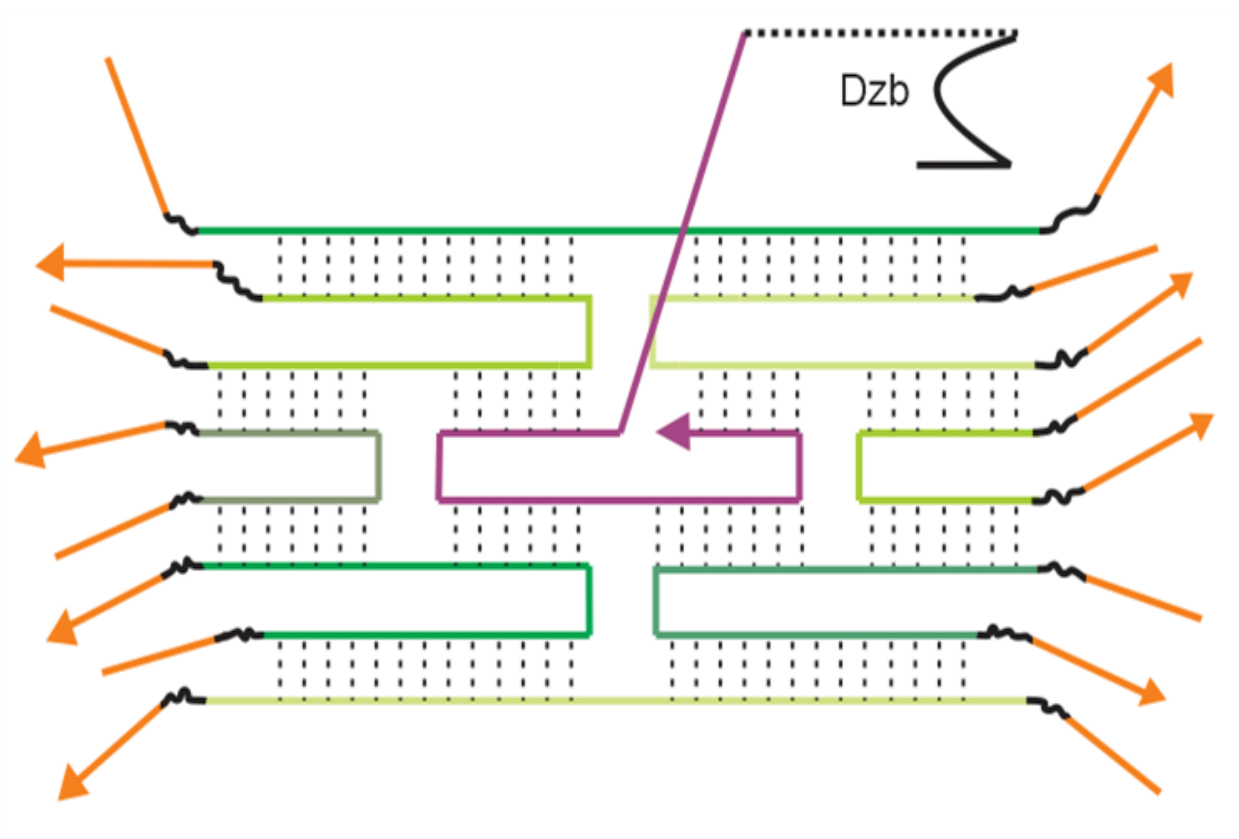


Figure 4. Deoxyribozyme (Dz) 10-23 associated on tile. **DZ_b** of Dz 10-23 is in the center attached to the tile by the middle, purple strand while **DZ_a** (Not shown) is dissolved in solution. Orange strands indicate nucleotide sequences (16 total) where the **hooks** can hybridize to the tile. Hooks not shown.

In total, there are 16 locations for the hooks to attach to the tile platform. The other half of the sequence in the hooks has affinity to the substrate. The **delivering hooks** have a sequence that does not match the binding region between the substrate and Dz 10-23. This prevents competitive binding. The **releasing hooks** do have affinity to the binding region between the substrate and Dz 10-23, which gives it affinity to the cleaved product. When substrate is added to the solution it is bounded to the tile by the **hooks**, which are randomly hybridized around the tile. This localizes the substrate around the DNAzyme reaction center on the tile without having to increase their overall concentration in solution, which would increase background fluorescence. The hooks are designed to be long enough to “deliver” substrate from the edge of the tile to the reaction center. This way

they could act similar to the swinging arm seen in Fu *et. al.*^[7] We then have the **releasing hooks**, which will “pull” the substrate away, releasing it from the reaction center after it is cleaved. See Figure 5 for reaction scheme. Notice that Figure 5A shows the initial reaction scheme of current Dz biosensors whereas Figure 5B shows the reaction scheme on the tile format created in this experiment. With this format, we hypothesize that this will allow the substrate and deoxyribozyme to bind together earlier, overcoming the current diffusion limitation for k_1 as well as for k_3 , and will push the limit of detection to below the current limit of detection (5pM).^[3]

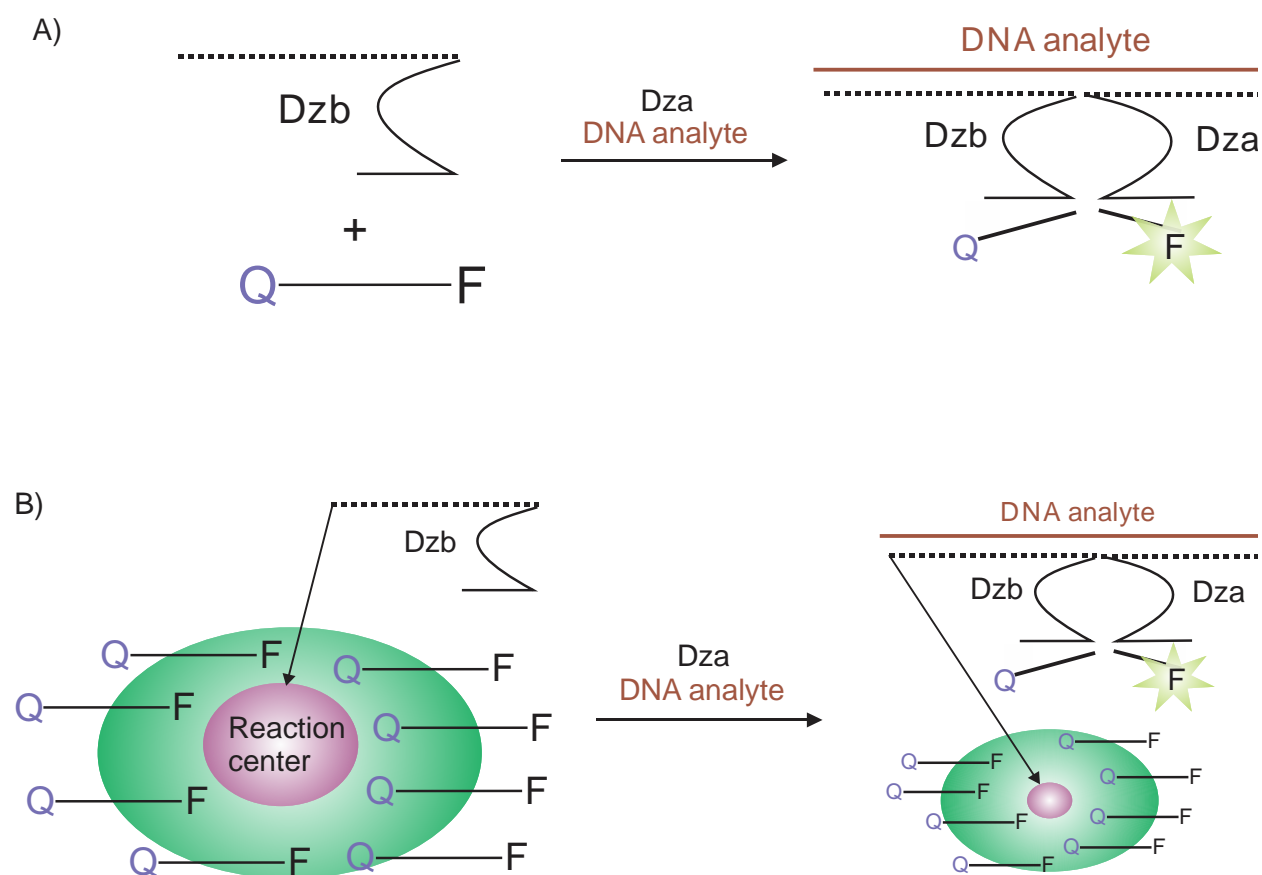


Figure 5 A) Reaction scheme of Dz 10-23 biosensor. **DZ_b** and the substrate are dissolved in solution. When **DZ_a** and the analyte are added to the solution, the analyte binds to the analyte binding arms (dotted lines). This brings the Dz reaction core together allowing for the substrate to bind, be cleaved by the Dz biosensor, and then fluoresce as the fluorophore and quencher separate. B) Arrangement of the Dz 10-23 biosensor on the antenna tile. **DZ_b** is attached to the tile by the analyte binding arms while substrate (shown by Q—F strands) is attached to hooks (not shown) on the tile and concentrated around the reaction center. Addition of **DZ_a** and analyte brings the Dz core together allowing for the substrate to bind, be cleaved by the Dz biosensor, and then fluoresce as the fluorophore and quencher separate.

Using the theories above, we annealed the tile and then tested its formation after being annealed, by running various forms of the tile on a native gel. The results of the gel are shown in Figure 6. Comparing Lane 2 and Lane 3 we see the addition of TDz 5 (the center strand that holds the **DZ_b**) increases the size of the tile, as expected. Lanes 4 and 5 show the increase in the size of the tile when the hooks are added to solution, therefore the hooks are also annealing around the tile complex. In lane 6, the Mtb analyte was added and we can see that the tile still forms in the presence of the analyte.

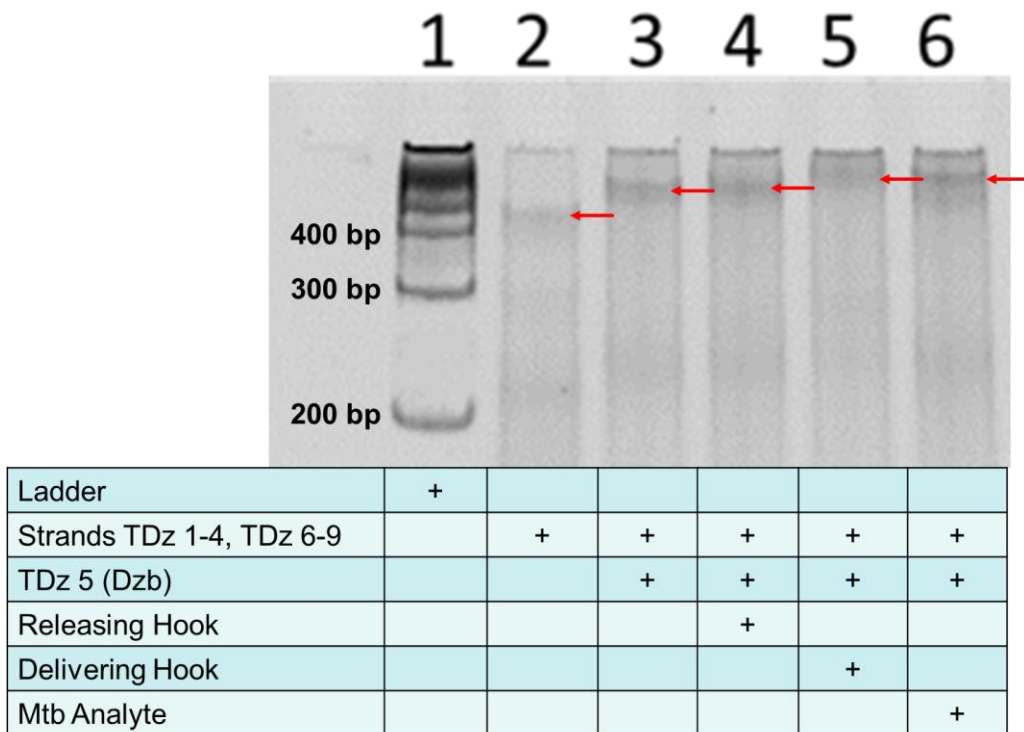


Figure 6 Native Gel electrophoresis of the samples. Lane 1 is the 100bp DNA ladder. Lane 2 is the Dz tile at 100 nM without Tdz5 (**DZ_b** of enzyme) and no hooks. Lane 3 is the full Dz tile at 100 nM with no hooks. Lane 4 is the full Dz tile at 100 nM with releasing hook at 160 nM. Lane 5 is the full Dz tile at 100 nM with delivering hook at 160 nM. Lane 6 is the full Dz tile at 100 nM with Mtb at 100 nM.

Confirming the LOD of Sensor Dissolved in Solution

In order to test the detection limit of the tile compared to the enzyme free in solution, the detection limit of the Dz 10-23 biosensor dissolved in solution had to be confirmed. The deoxyribozyme biosensor was split into two pieces, **DZ_a** (which was tested at 2 nM concentration) and **DZ_b** (which was tested at 10 nM concentration). After testing various concentrations of **DZ_a** and **DZ_b**, these concentrations showed the lowest change in background fluorescence between the substrate only and substrate with tile only, which is why they were chosen. The DNAzyme was placed in 200 nM solution of the F-substrate. The analyte, a synthetic DNA sequence that corresponds to a portion of 23S rRNA in Mtb, was added at 0 pM, 0.5 pM, 1 pM, 2 pM, 5 pM, 10 pM, 20 pM, and 100 pM concentrations. The fluorescence at 517nm was measured after 1 hr. and 3 hrs. with a fluorimeter and plotted against the analyte concentration. This experiment was completed three times. The threshold limit was set at 3 standard deviations above the fluorescence of our control (0 pM) and from that we calculated the limit of detection. Figures 7 shows the graphs of these results. The Limit of Detection was 25.68 pM after 1hr and 4.07 pM after 3 hrs.

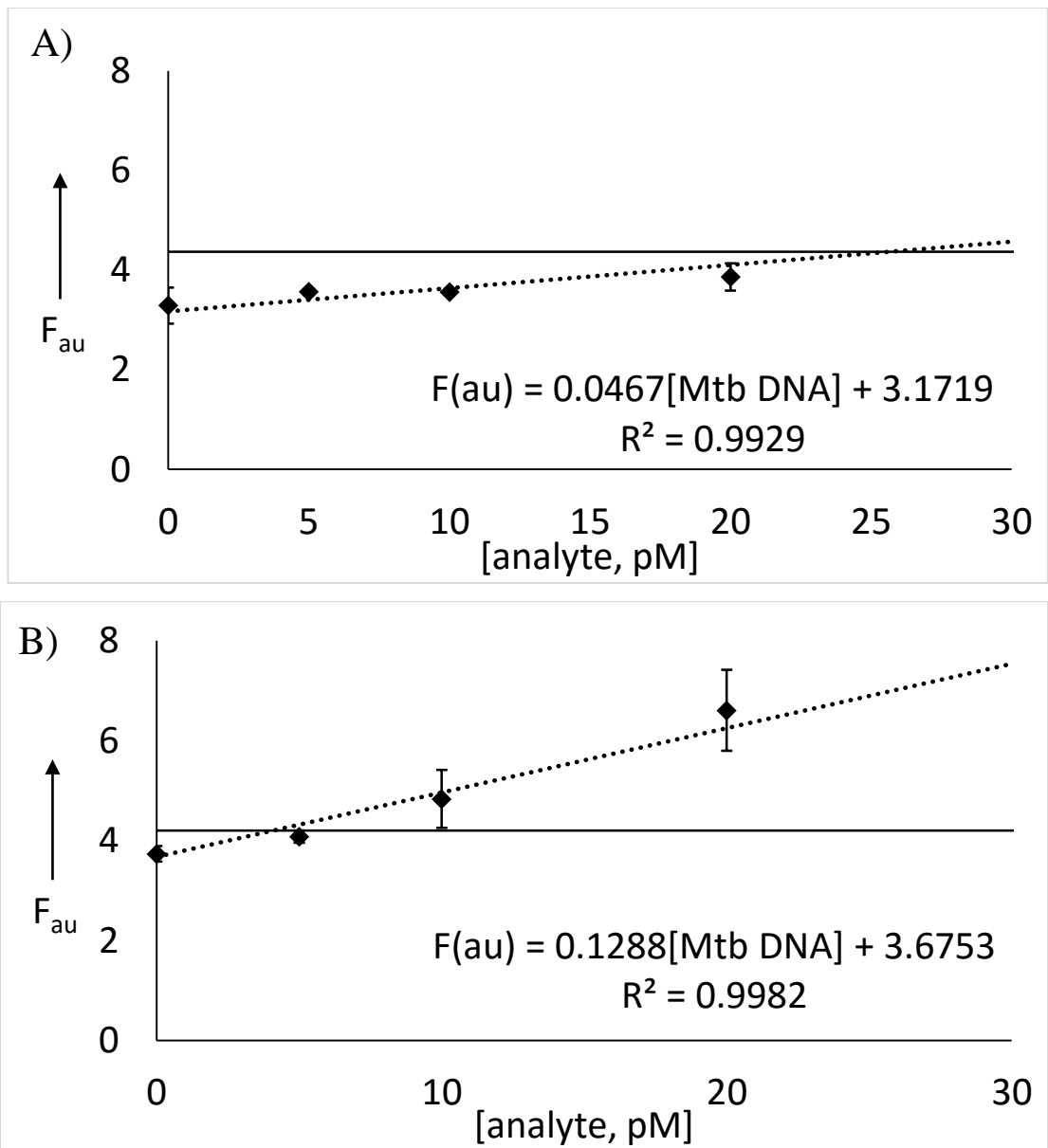


Figure 7 Deoxyribozyme 10-23 was dissolved in solution as two pieces. DZ_a concentration was 2 nM, DZ_b concentration was 10 nM, and F-substrate concentration was 200 nM. A) Absorbance at 517 nm of the sensor after 1 hr. of incubation at 55°C in the presence of various Mtb analyte concentrations. Limit of detection was 25.68 pM. B) Absorbance at 517nm of the sensor after 3 hrs. of incubation at 55°C in the presence of various Mtb analyte concentrations. Limit of detection was 4.07 pM. For both, the dashed lines show trendlines. Data are averages from three independent experiments and error bars show standard deviation. Solid line indicates threshold limits.

Testing the Tile Format

Using similar methods as listed above, we tested the limit of detection of the Dz 10-23 in the tile format. The same concentrations and analyte were used and we found the limit detection to be 2.31 pM after 1 hr and 0.51 pM after 3 hrs. The data for this is shown in Figure 8. For this reaction we did change the substrate to 1S-Hook. This substrate only differs from F-substrate in an extended sequence which is where the delivering hook binds to the substrate. This prevents competitive binding between the delivering hooks and the Dz 10-23 over the substrate. It also limits the linearization of the substrate, which was causing higher levels of background fluorescence.

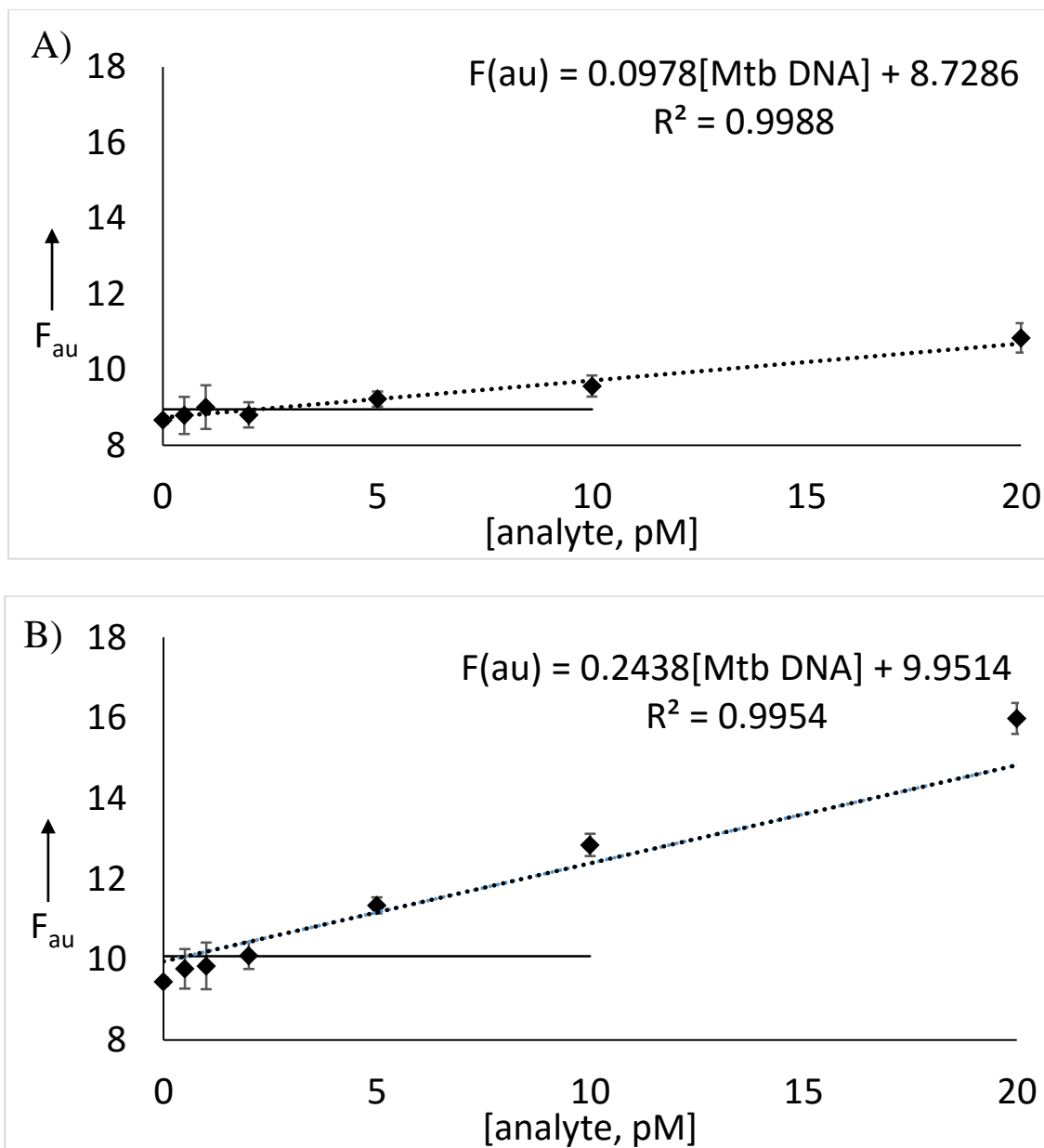


Figure 8 Deoxyribozyme 10-23 was dissolved in solution as two pieces. DZ_a concentration was 2 nM, DZ_b on the tile concentration was 10 nM, and 1S-Hook substrate concentration was 200 nM. Absorbance at 517 nm of the sensor after 1 hr. and 3 hrs. of incubation at 55°C respectively in the presence of various Mtb analyte concentrations. Dashed lines show trendlines. Data are averages from three independent experiments and error bars show standard deviation. Solid line indicates threshold limits. The Limit of detection was 2.31 pM after 1 hr. and 0.51 pM after 3 hrs.

To determine if the decreased detection limit was due to the channeling of the hooks and not some other interaction with the tile, we ran a control with the tile format and no hooks. The results of this are shown in Figure 9. From this figure, we see that the tile format without the hooks has a comparable slope (which is a measure of the DNAzyme's sensitivity to the substrate) to when the biosensor is dissolved in solution. When we compare the biosensor dissolved in solution slope with the slope of the tile format with both hooks, we see an increase in the sensitivity of the DNAzyme to its substrate. Therefore, we can infer that it is the addition of the hooks that changes the efficiency of Dz 10-23 Biosensor at detecting low levels of analyte.

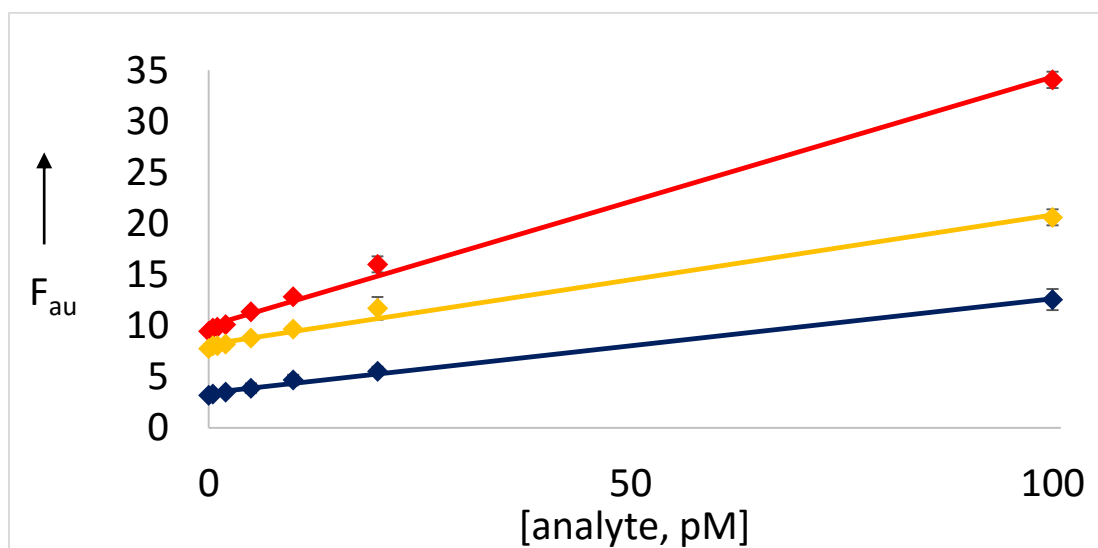


Figure 9 Deoxyribozyme 10-23 trendline comparisons after 3 hrs incubation at 55°C. DZ_a concentration was 2 nM, DZ_b concentration was 10 nM, Hook concentrations were both at 160 nM, and substrate concentration was 200 nM. Absorbance at 517 nm of the sensor was measured in presence of various Mtb analyte concentrations. Data are averages from three independent experiments and error bars show standard deviation. Free sensor in solution (Blue), Dz Tile with No Hooks (Yellow), and Dz Tile with both the **delivering hook** and **releasing hook** (Red).

Checking Selectivity

One of the main advantages of Dz biosensors and specifically of the design of the split biosensor, is that they are very selective since the hybridization is due to Watson-Crick base pairs forming. Even a single point mutation can decrease the melting temperature of the strand by several degrees Celsius. Therefore, to check that our tile format retained selectivity, we built a similar biosensor tile that was specific to *Mycobacterium smegmatis* (*M. smeg.*) which we will now call sensor 2. *M. smeg.* is a nonvirulent species of mycobacterium compared to *Mycobacterium tuberculosis* which causes tuberculosis in humans. Therefore, being able to differentiate between the two species is crucial in correctly diagnosing and treating patients. While *M. smeg* will not be in patient samples, it will serve as a model for our biosensor tile design differentiating between the different Mtb strains (antibiotic resistant vs. extremely antibiotic resistant, etc.) *M. smeg* has a similar 23S rRNA sequence with a few key mutations which should lower the activity of the Mtb biosensor since it is not the specific analyte, resulting in less fluorescence. In Figure 10 we compare the limit of detection of sensor 2 dissolved in solution versus in a tile format. This was to make sure that the Dz biosensor was indeed working correctly and would make a good comparison for selectivity of the Dz biosensors. In solution, the limit of detection was 6.40 pM while on tile the limit of detection was 1.91 pM. This confirmed similar decreases in limit of detection when the sensor was placed on the tile format, compared to when it was dissolved in solution.

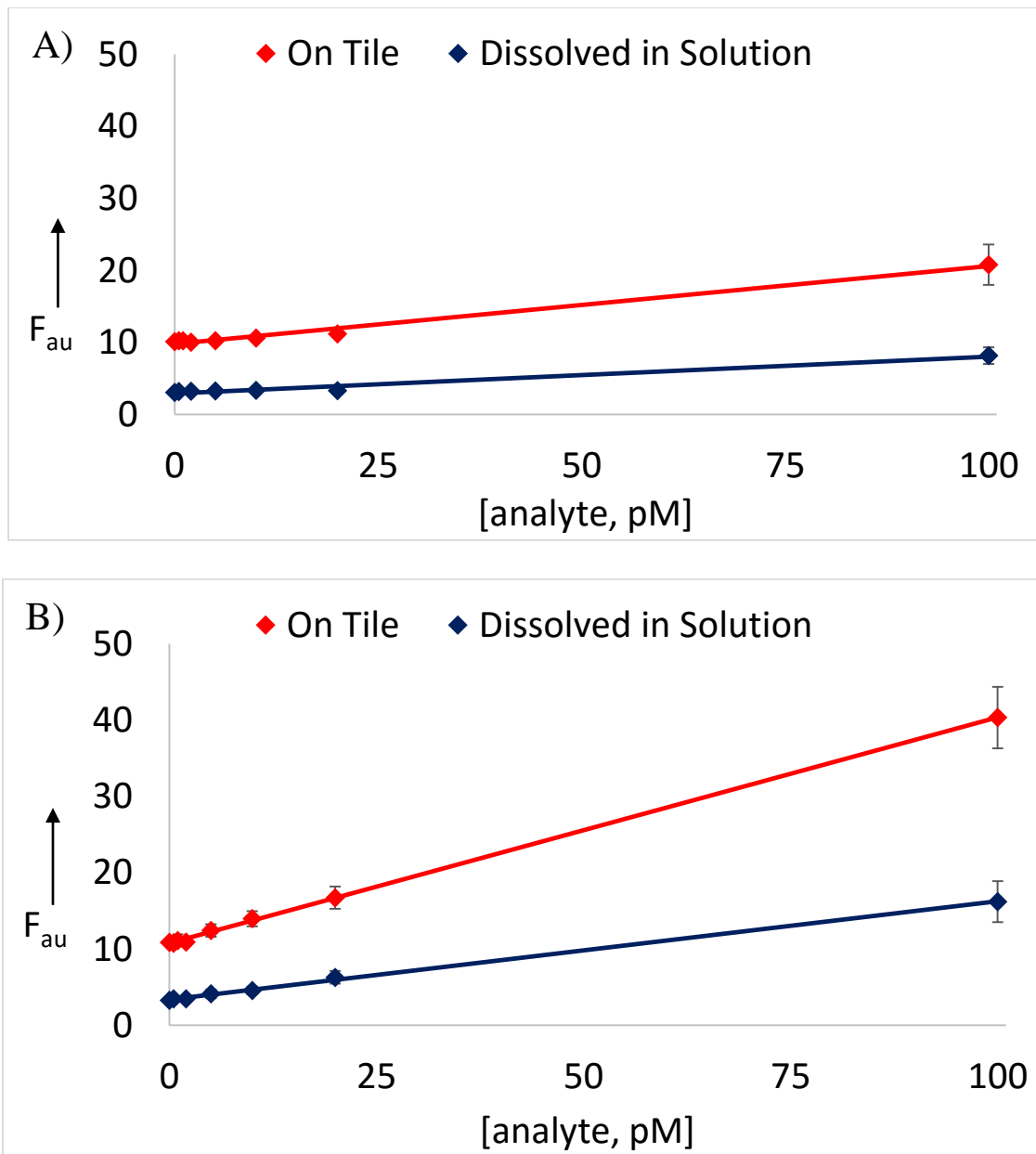


Figure 10 Limit of detection for sensor 2 dissolved in solution versus tile-associated Dz sensor 2 after 1 hr and 3 hrs. *M. smeg* **DZ_a** concentration was 2 nM, *M. smeg* **DZ_b** tile concentration was 10 nM, and substrate concentration was 200 nM. A) Absorbance at 517 nm of the sensor after 1 hr of incubation at 55°C in presence of various *M. smeg* analyte concentrations. Limit of detection was 15.21 pM for the sensor in solution and 11.63 pM on tile. B) Absorbance at 517 nm of the sensor after 3 hrs of incubation at 55°C in presence of various *M. smeg* analyte concentrations. Limit of detection was 6.40 pM in solution and 1.91 pM on tile. For both experiments, data are averages from three independent experiments and error bars show standard deviation.

We then measured the selectivity of the two sensors in tile format by measuring their fluorescence first when in the presence of their specific analyte and second with their nonspecific analyte. We measured this after 1 hr with the analyte concentrations at 100 pM. In Figure 11 we see that the tile sensors indeed remained selective to their specific analyte with higher fluorescence correlating to the matched analyte and lower fluorescence for the mismatched analyte.

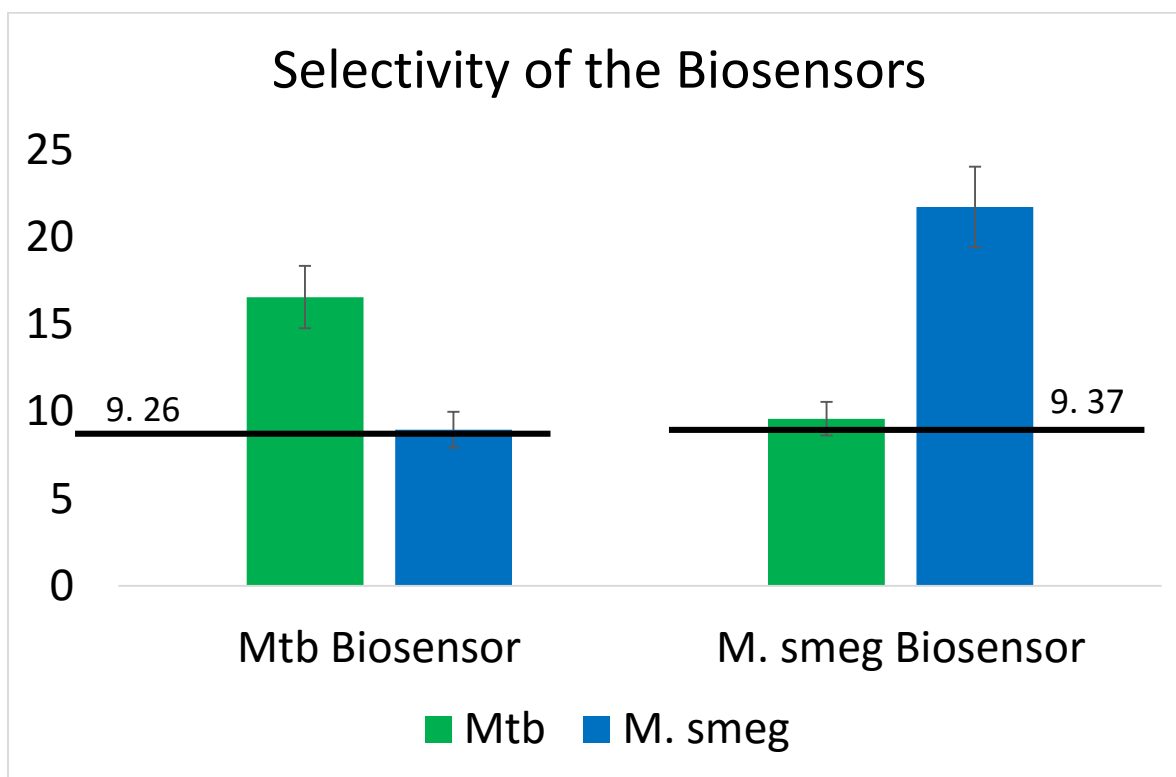


Figure 11 Shows the specificity of the Dz tile to its analyte Mtb and of Dz M. smeg tile to its analyte M. smeg. On the left is sensor 1 (Mtb sensitive biosensor) and on the right is sensor 2 (M. smeg sensitive biosensor). When sensor 1 is incubated with 100 pM of its matched analyte (Mtb, shown in green) for 1 hr, there is greater fluorescence than when sensor 1 was incubated with 100 pM of its mismatched analyte (M. smeg, shown in blue). For sensor 2, when incubated with its matched analyte (M. smeg) for 1 hr at 100 pM, there is greater fluorescence compared to when sensor 2 was incubated with its mismatched analyte (Mtb) for 1 hr at 100 pM.

Testing the Tile with RNA

Now that we have proved that our tile format of Dz 10-23 has lower detection limits and remains selective, we finally wanted to check how the tile functioned when the analyte sequence was from samples of rRNA instead of synthetic DNA. Up until this point, we had used Mtb in our testing which is a short fragment of synthetic DNA that corresponds to a portion of 23S rRNA in Mtb. To simulate real diagnostic tests, we wanted to measure the presence rRNA directly from samples. Therefore, we ran the same trials listed above with rRNA analyte that was extracted from BCG (Bacillus Calmette-Guerin). The results of these trials show a universal increase in the limit of detection for the tile and non-tile formats, with lower limits of detection still appearing in the tile format compared to the biosensor dissolved in solution, as seen in Figure 12. In solution, the limit of detection was 11.97 pM while the limit of detection on tile was 6.40 pM. Looking at research done by others, we inferred that the complexity of the secondary structure might be one reason for the increase in limit of detection in the deoxyribozyme biosensor.

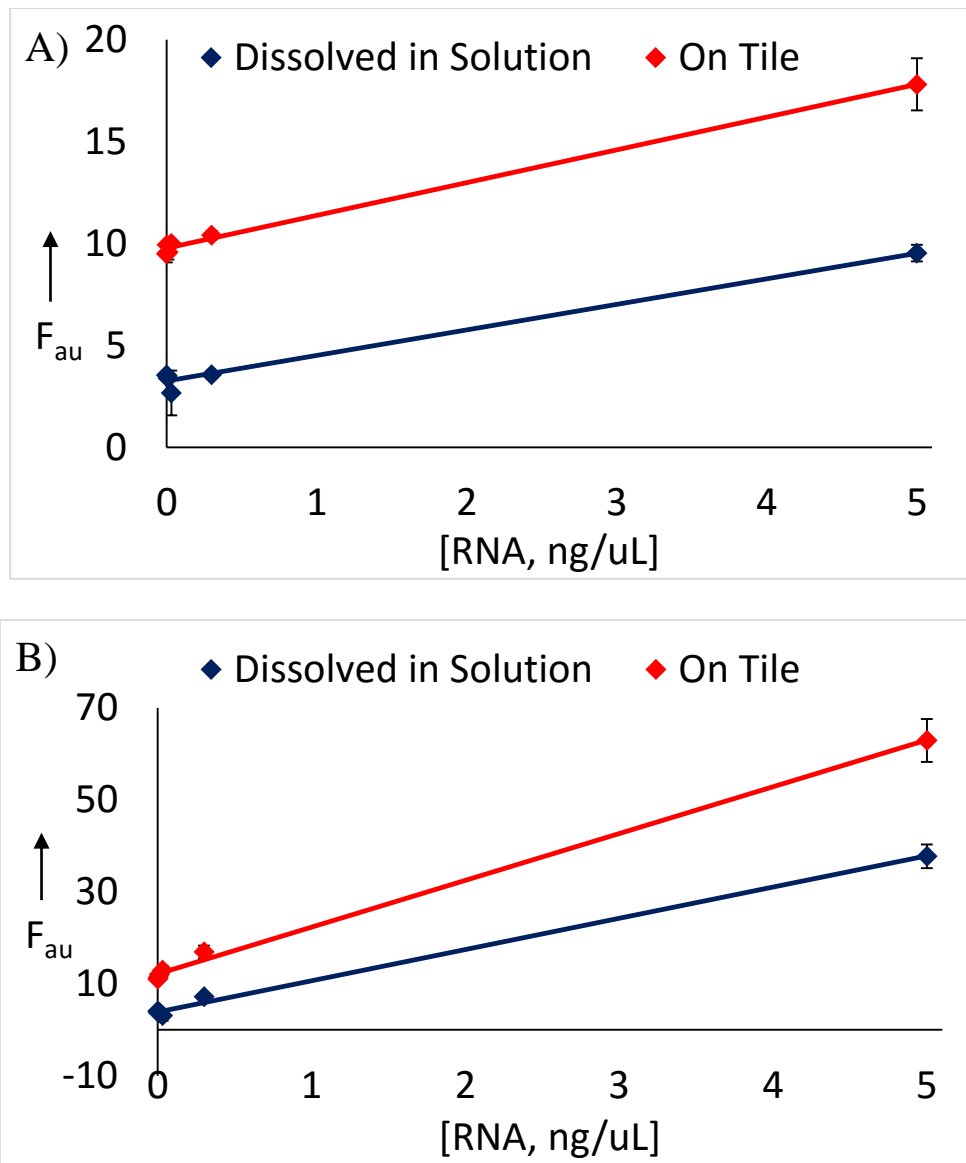


Figure 12 Shows the fluorescence measurements of the Dz tile with RNA analyte compared to the sensor dissolved in solution with the RNA analyte. The DZ_a was at 2 nM, DZ_b was at 10 nM and attached to the tile, hook concentrations were both at 160 nM, the substrate was at 200 nM, and the RNA analyte concentration varied. A) Sample was incubated at 55°C and the fluorescence at 517 nm read after 1hr. The limit of detection of the biosensor dissolved in solution was 24.73 pM and on tile was 38.46 pM. B) Sample was incubated at 55°C and the fluorescence at 517 nm read after 3hrs. The limit of detection of the biosensor dissolved in solution was 11.97 pM and on tile was 6.40 pM. For both experiments, the data is an average of three experiments and the standard deviation is represented by the error bars.

SUMMARY

We set out to design an environment around our Dz 10-23 biosensor that would optimize the reaction conditions to both improve the efficiency of the biosensor and lower the detection limits of Dz Biosensors. Figure 13 shows a table that compares the limits of detections measured for this experiment after 3 hrs and summarizes what we have found. From this we can conclude that placing the Dz 10-23 biosensor on a DNA antenna tile can lower detection limits, in some cases by 10 fold, while retaining selectivity of the tile. We also found that the Dz 10-23 biosensor on antenna tile works with both rRNA and DNA analytes. While the rRNA samples did show slightly higher limits of detection, we inferred that this may be due to secondary interactions and are currently looking into ways to reduce this difference. Having proven the basis of the idea and theory behind the hypothesis, we also are looking into further optimization of the tile to push the LOD even lower. With this information, we are now a step closer to perfecting deoxyribozyme biosensors to be used for diagnostic procedures in the field, as well as any other area where deoxyribozymes can be applied including treatment of disease, food and water contamination diagnostics, computational functions, etc.

		In solution (pM)	On Tile (pM)
Synthetic Analyte	Mtb Sensor	4.07	0.51
	M. smeg Sensor	6.40	1.91
RNA	Mtb Sensor	11.97	6.40

Figure 13 Shows the limits of detections after 3 hrs of incubation at 55°C for each experiment with a gradient showing the best and worst. From these experiments we can see that the tile format reduces the limits of detection.

LIST OF REFERENCES

- [1] Breaker, R.R., and Joyce, G.F. A DNA enzyme that cleaves RNA. *Chem. Bio.* (1994) **1**, 223-229
- [2] Schlosser, K., Li, Y. Biologically inspired synthetic enzymes made from DNA. *Chemistry & Biology.* (2009) **16**, 311-322. DOI: 10.1016/j.chembiol.2009.01.008
- [3] Mokany, E., Bone, S.M., Young, P.E., Doan, T.B., Todd, A.V. MNazymes, a versatile new class of nucleic acid enzymes that can function as biosensors and molecular switches. *J. AM. Chem. Soc.* (2010) **132**, 1051-1059. DOI: 10.1021/ja9076777
- [4] Gerasimova, Y.V., Cornett, E.M., Edwards, E., Su, X., Rohde, K.H., Kolpashchikov, D.M. Deoxyribozyme cascade for visual detection of bacterial RNA. *ChemBioChem.* (2013) **14**, 2087-2090. DOI: 10.1002/cbic.201300471
- [5] Santoro, S.W., Joyce G.F. A general purpose for RNA-cleaving DNA enzyme. *Proc. Natl. Acad. Sci. U.S.A.* (1997) **94**, 4262-4266.
- [6] Santoro, S.W., Joyce G.F. Mechanism and utility of an RNA-cleaving DNA enzyme. *Biochemistry* (1998) **37**, 13330-13342.
- [7] Fu, J., Yang, Y.R., Johnson-Buck, A., Liu, M., Liu, Y., Walter, N.G., Woodbury, N.W., Yan, H. Multi-enzyme complexes on DNA Scaffolds capable of substrate channeling with an artificial swinging arm. *Nature Nanotechnology.* (2014) **9**, 531-536. DOI: 10.1038/NNANO.2014.100
- [8] Gerasimova, Yulia V., Kolpashchikov, Dmitry M. Folding of 16S rRNA in a Signal-Producing Structure for the Detection of Bacteria. *Angew. Chem. Int. Ed.* (2013) **52**, 1-6. DOI: 10.1002/anie.201303919
- [9] Baum, D.A., Silverman, S.K. Deoxyribozymes: useful catalysts in vitro and in vivo. *Cell. Mol. Life Sci.* (2008) **65**, 2156-2174. DOI: 10.1007/200018-008-8029-y

- [10] Dass, Crispin R., Choong, Peter F.M., Khachigian, Levon M. DNzyme technology and cancer therapy: cleave and let die. *Mol. Cancer Ther.* (2008). **7**, 243-251.
- [11] Stojanovic, Milan N., Prada, Paloma de, Landry, Donald W., Catalytic Molecular Beacons. *Chem.Bio.Chem.* (2001) **2**, 411-415.
- [12] Reed. Lester J. Multienzyme complexes. *Acc. Chem. Res.* (1974) **7**:40-46
- [13] Kolpashchikov, D.M. *ChemBioChem.* (2007) **8**, 2039-2042